Since January 2020 Elsevier has created a COVID-19 resource centre with free information in English and Mandarin on the novel coronavirus COVID-19. The COVID-19 resource centre is hosted on Elsevier Connect, the company's public news and information website.

Biochemical and Biophysical Research Communications 419 (2012) 137–141

Contents lists available at SciVerse ScienceDirect

Biochemical and Biophysical Research Communications

journal homepage: www.elsevier.com/locate/ybbrc

Biophysical characterisation of the nucleocapsid protein from a highly pathogenic porcine reproductive and respiratory syndrome virus strain

Stefanie S. Jourdan [a], Fernando A. Osorio [b], Julian A. Hiscox [a,*]

[a] Institute of Molecular and Cellular Biology, Faculty of Biological Sciences, Astbury Centre for Structural Molecular Biology, University of Leeds, Leeds LS2 6JP, UK
[b] School of Veterinary and Biomedical Sciences, Nebraska Centre for Virology, University of Nebraska-Lincoln, NE 68583-0900, USA

ARTICLE INFO

Article history:
Received 11 November 2011
Available online 28 January 2012

Keywords:
Porcine reproductive and respiratory syndrome virus
PRRSV
Nucleocapsid protein
Biophysical
RNA binding

ABSTRACT

The arterivirus nucleocapsid (N) protein is a multifunctional protein that binds viral RNA for encapsidation and has potential roles in host cell processes. This study characterised the N protein from a highly virulent North American strain of porcine reproductive and respiratory syndrome virus (PRRSV). The association with viral RNA was mapped to defined motifs on the N protein. The results indicated that disulphide bridge formation played a key role in RNA binding, offering an explanation why infectious virus cannot be rescued if cysteine residues are mutated, and that multiple sites may promote RNA binding.

1. Introduction

Coronaviruses and arteriviruses are families of positive strand RNA viruses that replicate in the cytoplasm of an infected cell. Due to similar genome organisation, replication and transcription strategies these viruses are grouped together into the *Nidovirales*. Many of their members cause important respiratory, gastrointestinal and reproductive diseases. These include severe acute respiratory syndrome coronavirus (SARS-CoV) [1], a zoonotic infection of humans and animals, and the arterivirus porcine reproductive and respiratory syndrome virus (PRRSV) that causes reproductive failure in pregnant sows, high mortality in piglets and respiratory disease in pigs of any age [2,3]. Although vaccines to a number of coronaviruses and arteriviruses exist, the high mutation rates during virus replication leads to new viral threats that are constantly emerging [4]. A more molecular understanding of viral protein function would allow the development of new vaccines, identify targets for targeted antiviral therapy and provide robust diagnostics [5,6].

The PRRSV genome shows rapid change and strains can vary in virulence [7], with various genes contributing to pathogenesis, including the nucleocapsid (N) protein [8–10]. For both the coronaviruses and arteriviruses the N protein is one of the most abundant virally encoded proteins and plays essential roles in the virus life cycle [11,12]. Its most prominent role is complexing with viral RNA, although the mechanisms for this for either type of viral N protein is not precisely characterised. For the coronavirus N protein phosphorylation has been shown to play a role in mediating binding to RNA [13,14] with the amino-terminal region facilitating long-range non-specific electrostatic interactions potentially allowing contacts to form via a 'lure' and 'lock' mechanism [15].

Sequence comparison initially suggested that coronavirus N proteins exhibited a three-domain structure. This includes a disordered unstructured region at the N-terminal end that is followed by the structured N-terminal domain (NTD). A disordered serine/arginine- (SR-) rich region is located in the central position of the coronavirus N protein. Similarly the extreme C-terminus is disordered with a proximally structured C-terminal domain (CTD). The arterivirus N proteins are smaller in size with regard to molecular weight (the coronavirus N protein is approximately 45 kDa whereas the arterivirus N protein is approximately 15 kDa) and consists of an N-terminal half that is mainly disordered and a structured C-terminal half which has a similar fold as the CTD of the coronaviruses [16]. Due to the abundance of disordered regions in combination with proteolytic instability of the full length N proteins [17] the detailed structure of the N protein has not been solved in entirety using any one single technique and our picture of this is based on multiple complementary analyses.

The X-ray structures of the CTD of the arterivirus equine arteritis virus (EAV) and PRRSV N proteins have been solved and show structural similarities to the CTD of the coronavirus N protein [16,18,19]. There is a very high overall similarity between the CTD of EAV and PRRSV N proteins. The main differences exist in

* Corresponding author. Address: Room 8.58, Garstang Building, Institute of Molecular and Cellular Biology, Faculty of Biological Sciences, University of Leeds, Leeds LS2 9JT, UK. Fax: +44 113 343 5638.
E-mail address: j.a.hiscox@leeds.ac.uk (J.A. Hiscox).

0006-291X/$ - see front matter © 2011 Elsevier Inc. All rights reserved.
doi:10.1016/j.bbrc.2011.11.126

their β-loops and their most C-terminal α-helices that end about 6 residues before the C-terminus. Monomers of EAV and PRRSV N harbour two anti-parallel β-strands that are flanked by two α-helices. Both proteins contain another short α-helix towards the N-terminal of the CTD. Moreover, PRRSV as well as EAV N are predicted to contain an α-helix within their otherwise unstructured N-terminal half. Similar to the coronavirus N proteins EAV and PRRSV N form dimers with a β-sheet platform that is surrounded on one side of the dimer by the α-helices. With a view to potential RNA binding or other interactions taking advantage of electrostatic interactions, the electrostatic potential is more positive on the side of the dimer on which the helices reside. The proposed RNA binding region of the PRRSV N protein, based on the structure, is in the unstructured N-terminal half, located within a region harbouring positively charged residues. With a negative electrostatic potential found on the side of the β-sheet floor this could support correct positioning of the RNA in complex to N protein. PRRSV N is found in a head to head helical arrangement within the crystals, supporting the ribbon-like pattern observed for N using cryo-tomography [20].

To provide a deeper understanding of the role of PRRSV N protein in binding RNA and to delineate RNA binding regions a sequential alanine substitution approach was used in combination with various biophysical assays and selected further point mutation. This analysis highlighted that several sites on the PRRSV protein may act cooperatively to promote RNA binding.

2. Materials and methods

2.1. Bacterial strains and construction of plasmids

The N gene from PRRSV strain NVSL #97-7895 was cloned into the pTriEx1.1Neo (Novagen) vector. Alanine block substitutions were constructed by a two-step PCR approach creating products allowing for a triple ligation with the pTriEx1.1Neo vector. Plasmid pTriExN_{C23S} coding for an N protein carrying a cysteine (cys) to serine mutation at residue 23 was created by site directed mutagenesis.

2.2. Protein expression and purification

Plasmids coding for N protein variants were transformed into Tuner (DE3) pLacI (Novagen) *E. coli* cells that allowed for efficient protein expression.

2.3. Gel filtration chromatography

Aliquots of purified protein were analysed by analytical gel filtration chromatography (GFC) using a BioSep-Sec-S3000 column (Phenomenex) at a flow rate of 0.8 ml/min of the mobile phase; 20 mM Tris HCl pH 7, 0.5 M NaCl. Protein standards were used to establish a standard curve; Cytochrome C (12.4 kDa), carbonic anhydrase (20 kDa), bovine serum albumin (66 kDa), β-amylase (200 kDa), catalase (210 kDa), Dextran blue (2000 kDa). The molecular mass of the contents of the peak eluting upon N protein injection was estimated from its retention time using the standard curve.

2.4. Circular dichroism (CD)

Proteins used in CD analysis were purified without the addition of reducing agents and treated with high RNase A concentrations so that no RNA was co-purified. Prior to CD analysis proteins were dialysed into buffer containing 20 mM sodium phosphate pH 7.0 and 0.3 M or 0.5 M sodium fluoride. CD data was analysed using Dichroweb [21] (http://dichroweb.cryst.bbk.ac.uk/html/home.shtml) similar to that described for the coronavirus N protein [15].

3. Results and discussion

3.1. The N protein interacts with RNA

To investigate RNA binding and establish an *in vitro* RNA binding assay for the N protein, the N gene from an infectious cDNA of the highly lethal North American PRRSV strain NVSL #97-7895 [22] was cloned into the expression vector pTriEx1.1Neo (Novagen) and the recombinant protein purified from *E. coli* using metal affinity chromatography as described [13]. RNA co-purification was used to indicate the RNA binding capability of N protein. The amount of RNA that could be extracted from an equal amount of purified protein decreased when the protein was incubated with increased RNase A concentration (Fig. 1A). To control for protein stability, protein samples were taken at the end of the incubation and analysed by SDS–PAGE (Fig. 1A).

The size of the co-purified RNA was estimated by electrophoretic analysis and a major species found to be approximately 150 nucleotides. To investigate whether the 150 nucleotides were bound by one N protein molecule, analytical gel filtration chromatography (GFC) was performed (Fig. 1B). These molecular weights indicated that the two peaks contained multimers and possibly monomers, respectively. From the mass deduced from the elution time it is tempting to speculate that peak 1 represents a decamer, suggesting that each monomer protected an average of 15 nt from nucleolytic cleavage.

3.2. Global structure of the PRRSV N protein

No complete structure for the PRRSV N protein is available, therefore a combination of modelling using the sequence encompassing the CTD of the N protein from the VR-2332 strain was used to map the equivalent region on the NVSL #97-7895 strain N protein using the HHPred program (pdb file 1p65; http://toolkit.tuebingen.mpg.de/hhpred) and the secondary structure prediction program Jpred (http://www.compbio.dundee.ac.uk/www-jpred/) was employed to model potential folds within the N-terminal half (NTH) (Fig 2A). Overall the structure was confirmed using CD (Fig. 2B). For example, these suggested 15% alpha helix, 29% beta sheet and 56% random coil by the K2d neural network programme.

3.3. Potential role of disulphide bridge formation in RNA binding

The North American PRRSV N protein contains three cys residues at positions 23, 75 and 90 and has been shown to be present as disulphide-linked dimers in virions [23,24]. However, only equivalents of Cys23 and Cys75 are present within N proteins from European PRRSV strains. Cys23 and Cys90 may play an important role for in the virus life cycle as substitution of these residues with serine in recombinant infectious virus led to abrogation of progeny virus production [25]. To determine whether the cys residues had possible roles in mediating RNA binding, N protein was purified under reducing conditions and resulted in less RNA being co-purified (Fig. 3A). This indicated that the formation of disulphide linkages may play a role in RNA binding. Examination of the predicted N protein structure (Fig. 2A) indicated that Cys75 and Cys90 are too far away from their partners in the partial crystal structure to form disulphide bridges [19]. The possible role of Cys23 in RNA-binding was investigated by substituting this residue with serine (mutant N_{C23S}), and resulted in co-purification of no or very small amounts of RNA (Fig. 3B).

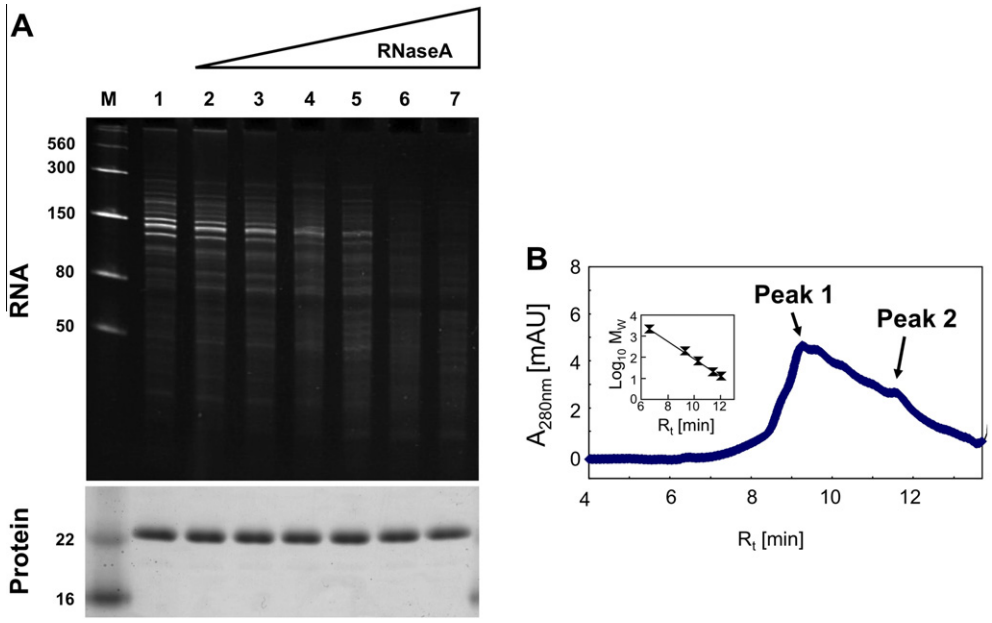

Fig. 1. RNA binding by the N protein. (A) Ethidium bromide stained acrylamide gel loaded with RNA extracted from equal amounts of purified recombinant N protein. Lanes 1, 2, 3, 4, 5, 6 and 7 contain RNA extracted from protein samples treated with 0, 5, 10, 20, 40, 80 and 160 ng/ml RNase A for 10 min at 30 °C, respectively. Sizes of the ssRNA marker are indicated on the left. Below the RNA gel, protein samples taken just prior to RNA extraction and analysed by SDS–PAGE are shown as control for protein stability during RNase A treatment. (B) Chromatogram obtained during analytical gel filtration chromatography of the N protein (blue trace). The inset shows the standard curve used to estimate the molecular weight of the species within the peak. The position of peaks potentially containing deca- (Peak 1) and monomers (Peak 2) of N protein are indicated by arrows. Both graphs have the retention time (R_t) plotted on the *x*-axis. The *y*-axis contains information about the absorbance units and logarithmic molecular weights for the N protein graph and the standard curve, respectively. (For interpretation of the references to colour in this figure legend, the reader is referred to the web version of this article.)

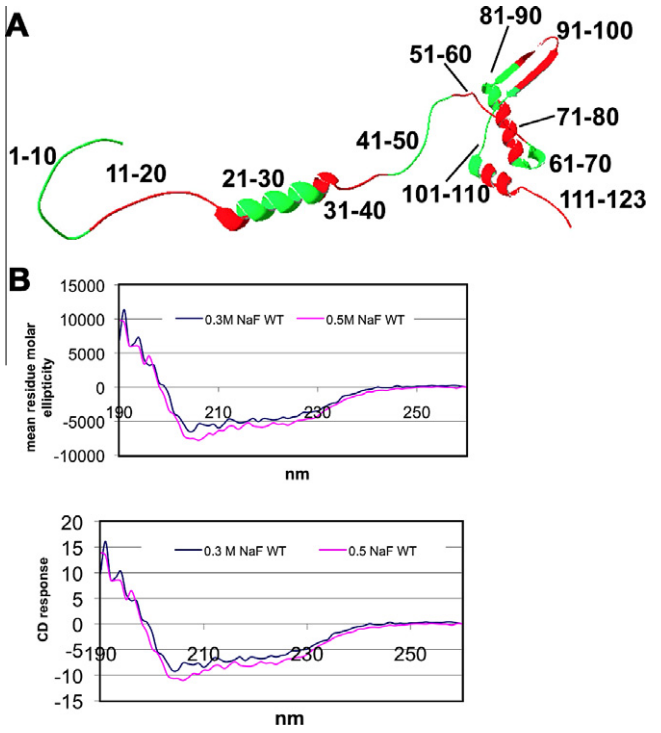

Fig. 2. (A) Predicted structure of PRRSV N protein which harbours one structured domain that is located in the C-terminal half. The N-terminal half of the protein is thought to be mainly unstructured besides a predicted α-helix. Shading in alternating red and green shows the positioning of the alanine block substitutions (corresponding to those in Table 1) used in this study on the predicted structure. (B) Representative CD spectra of the PRRSV protein in different concentrations of NaF. (For interpretation of the references to colour in this figure legend, the reader is referred to the web version of this article.)

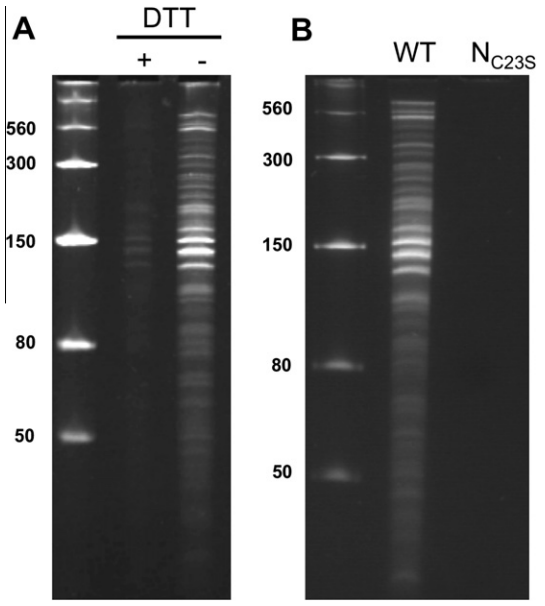

Fig. 3. RNA binding is influenced by disulphide bond formation. Shown are denaturing acrylamide gels onto which RNA was loaded which was extracted from equal amounts of protein. (A) RNA extracted from wild type N protein purified under reducing (+DTT) or non-reducing (−DTT) conditions. (B) RNA extracted from wild type N protein and the cys to serine mutant N_{C23S} that were purified under non-reducing conditions. Sizes of marker bands are indicated on the left of the panels.

The influence of disulphide bridge formation on RNA binding may be due to a higher valency that is achieved upon N protein

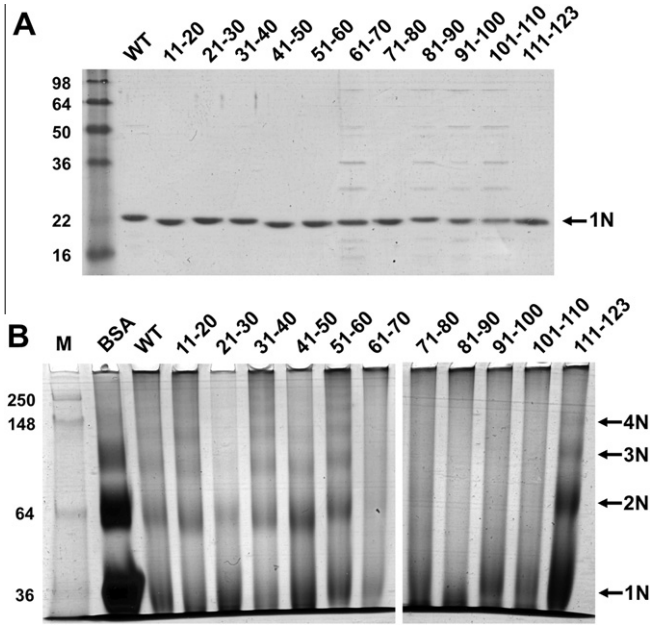

Fig. 4. Oligomerization by the N protein. (A) Assessment of purity of purified recombinant proteins. Coomassie stained SDS–PAGE gel loaded with approximately equal amounts of the wild type and alanine block substitutions. The sizes of marker bands are indicated to the left of the panel whereas to the right of the panel an arrow indicates the position of the N protein monomer (1 N). Positions of the alanine substitutions on each N protein are indicated above the panel. (B) Blue native gel onto which 2 μg of WT and mutant N proteins were loaded. On the left a protein marker as well as 5 μg of BSA were loaded. The identity of samples loaded is shown above each lane and the oligomeric state of protein complexes is indicated on the right of the panel.

oligomerization and stabilization by intermolecular disulphide bridges: A single N protein may only have one RNA binding site of low affinity, whereas oligomerization may lead to the availability of several RNA binding sites that could interact with the same RNA molecule. Multi-valency is a known means to increase the affinity of low affinity binding partners [26–28]. The suggested arrangement of N protein in the ribonucleocapsid leads to the close proximity of the positively charged regions surrounding the α-helix within the NTH of the protein [20,29]. Cys23 is contained within this α-helix and therefore may stabilize this arrangement upon formation of disulphide bridges. Alternatively, mutation of Cys23 may have disrupted other functions of the protein in terms of overall structure and underlying RNA binding signals.

3.4. The CTD is important for dimer formation whereas Cys23 stabilizes higher oligomers

To investigate whether other regions of the N protein interacted to promote RNA binding, an alanine block substitution approach was adopted. Each protein variant had sequentially 10 residues mutated into alanines. Each substituted block is indicated in the predicted structure of N protein (Fig. 2A), and the predicted structure and electrostatic potential of each variant protein is shown in Supplementary (Fig. S1). As the oligomeric state and valency of molecules can influence binding affinity the mutant N proteins were assessed with regard to their oligomeric state. Wild type N protein as well as the mutants were purified under non-reducing conditions and high RNase A concentrations to prevent co-purification of RNA. RNA has previously been shown to influence the oligomeric state of N protein [24]. To assess size and purity of the recombinant proteins, samples were analysed by SDS–PAGE (Fig. 4A). Due to the highly charged character of the N protein some of the alanine substitutions that cause a change in the charge of the protein resulted in different electrophoretic mobility.

To assess the oligomeric state under native conditions, the purified proteins were separated on native blue gels (Fig. 4B), allowing electrophoretic analysis under native conditions of proteins with high isoelectric points (pIs). N protein showed monomers, dimers, trimers and tetramers. Mutant N_{21-30} lacking Cys23 had a different migration pattern. This mutant is mainly present as monomer and dimer suggesting that Cys23 was involved in the formation of higher order oligomers. Alanine blocks within the well-structured CTH had a more dramatic effect on oligomer formation of N protein: Mutants N_{61-70}, N_{71-80}, N_{81-90}, N_{91-100} and $N_{101-110}$ showed significantly less discrete staining. Mutants N_{71-80}, N_{81-90}, N_{91-100} and $N_{101-110}$ were mainly present as monomers. Together with the finding that N_{31-40} could form oligomers indicated that amino acids 30–37 constituted not the only polypeptide sequence needed for dimer formation but that the CTH of N protein plays the main role in this process. As has been suggested by the crystal structure of the CTH.

3.5. Role of amino acid motifs in RNA binding

To investigate the role of different amino acids in RNA binding, the alanine block mutants were purified under non-reducing conditions that allowed co-purification of RNA with wild type N protein. RNA was extracted from purified proteins and compared to the amount extracted from equal amounts of wild type N protein. Table 1 summarises the results of this experiment. No RNA was co-purified with mutants N_{21-30}, N_{41-50} and $N_{111-123}$ indicating that residues within these regions may play a role in RNA binding. Yoo et al. [31] identified the region between residues 37 and 57 as containing RNA binding activity. The alanine block of mutant N_{41-50} is located within this region and specifically covers a region with a number of charged residues. It is possible that these positively charged residues bind to the negatively charged phosphate backbone of RNA. The alanine block of mutant N_{21-30} is not located within the previously identified RNA binding region. However, it is located within the predicted α-helix within the NTH of the protein (Fig. 2A). Moreover, mutant N_{21-30} harbours Cys23 whose mutation affects RNA binding. Also mutant $N_{111-123}$ did not co-purify any RNA. As deletions of the last 11 residues of PRRSV N protein influence its conformation [30], indicating that conformational changes may inhibit RNA binding.

In summary, PRRSV N protein contains a number of different functional sites involved in both recognition of viral RNA, sub-cellular localisation and interactions with other viral and cellular proteins [12,31]. Rather than individual motifs acting in isolation, both oligomerisation of the N protein and direct RNA binding motifs are likely to act in concert to promote RNA binding.

Table 1
RNA binding of N protein variants. The amount of RNA binding is indicated with + and − signs where a triple +++ indicates high binding affinity. ND, not determined.

	WT	N_{11-20}	N_{21-30}	N_{31-40}	N_{41-50}	N_{51-60}	N_{61-70}	N_{71-80}	N_{81-90}	N_{91-100}	$N_{101-110}$	$N_{111-123}$
RNA co-purified	+++	+	–	++	–	+	++	+	++	+	ND	+/–

Acknowledgment

This work was funded by a National Pork Board grant to FAO and JAH.

Appendix A. Supplementary data

Supplementary data associated with this article can be found, in the online version, at doi:10.1016/j.bbrc.2011.11.126.

References

[1] J.S. Peiris, K.Y. Yuen, A.D. Osterhaus, K. Stohr, The severe acute respiratory syndrome, N. Engl. J. Med. 349 (2003) 2431–2441.
[2] J.J. Meulenberg, PRRSV, the virus, Vet. Res. 31 (2000) 11–21.
[3] P.G. Plagemann, Porcine reproductive and respiratory syndrome virus: origin hypothesis, Emerg. Infect. Dis. 9 (2003) 903–908.
[4] E. Mateu, I. Diaz, The challenge of PRRS immunology, Vet. J. 177 (2008) 345–351.
[5] K.A. Spencer, F.A. Osorio, J.A. Hiscox, Recombinant viral proteins for use in diagnostic ELISAs to detect virus infection, Vaccine 25 (2007) 5653–5659.
[6] M. de Lima, B. Kwon, I.H. Ansari, A.K. Pattnaik, E.F. Flores, F.A. Osorio, Development of a porcine reproductive and respiratory syndrome virus differentiable (DIVA) strain through deletion of specific immunodominant epitopes, Vaccine 26 (2008) 3594–3600.
[7] C.C. Chang, K.J. Yoon, J.J. Zimmerman, K.M. Harmon, P.M. Dixon, C.M. Dvorak, M.P. Murtaugh, Evolution of porcine reproductive and respiratory syndrome virus during sequential passages in pigs, J. Virol. 76 (2002) 4750–4763.
[8] D. Yoo, C. Song, Y. Sun, Y. Du, O. Kim, H.C. Liu, Modulation of host cell responses and evasion strategies for porcine reproductive and respiratory syndrome virus, Virus Res. 154 (2010) 48–60.
[9] C. Lee, D. Hodgins, J.G. Calvert, S.K. Welch, R. Jolie, D. Yoo, Mutations within the nuclear localization signal of the porcine reproductive and respiratory syndrome virus nucleocapsid protein attenuate virus replication, Virology 346 (2006) 238–250.
[10] Y. Pei, D.C. Hodgins, C. Lee, J.G. Calvert, S.K. Welch, R. Jolie, M. Keith, D. Yoo, Functional mapping of the porcine reproductive and respiratory syndrome virus capsid protein nuclear localization signal and its pathogenic association, Virus Res. 135 (2008) 107–114.
[11] J.H. You, G. Howell, A.K. Pattnaik, F.A. Osorio, J.A. Hiscox, A model for the dynamic nuclear/nucleolar/cytoplasmic trafficking of the porcine reproductive and respiratory syndrome virus (PRRSV) nucleocapsid protein based on live cell imaging, Virology 378 (2008) 34–47.
[12] R.R. Rowland, R. Kerwin, C. Kuckleburg, A. Sperlich, D.A. Benfield, The localisation of porcine reproductive and respiratory syndrome virus nucleocapsid protein to the nucleolus of infected cells and identification of a potential nucleolar localization signal sequence, Virus. Res. 64 (1999) 1–12.
[13] H. Chen, A. Gill, B.K. Dove, S.R. Emmett, F.C. Kemp, M.A. Ritchie, M. Dee, J.A. Hiscox, Mass spectroscopic characterisation of the coronavirus infectious bronchitis virus nucleoprotein and elucidation of the role of phosphorylation in RNA binding using surface plasmon resonance, J. Virol. 79 (2005) 1164–1179.
[14] K.A. Spencer, M. Dee, P. Britton, J.A. Hiscox, Role of phosphorylation clusters in the biology of the coronavirus infectious bronchitis virus nucleocapsid protein, Virology 370 (2008) 373–381.
[15] K.A. Spencer, J.A. Hiscox, Characterisation of the RNA binding properties of the coronavirus infectious bronchitis virus nucleocapsid protein amino-terminal region, FEBS Lett. 580 (2006) 5993–5998.
[16] I.M. Yu, M.L. Oldham, J. Zhang, J. Chen, Crystal Structure of the Severe Acute Respiratory Syndrome (SARS) coronavirus nucleocapsid protein dimerization domain reveals evolutionary linkage between corona- and arteriviridae, J. Biol. Chem. 281 (2006) 17134–17139.
[17] H. Jayaram, H. Fan, B.R. Bowman, A. Ooi, J. Jayaram, E.W. Collisson, J. Lescar, B.V.V. Prasad, X-ray structures of the N- and C-terminal domains of a coronavirus nucleocapsid protein: implications for nucleocapsid formation, J. Virol. 80 (2006) 6612–6620.
[18] A. Deshpande, S. Wang, M.A. Walsh, T. Dokland, Structure of the equine arteritis virus nucleocapsid protein reveals a dimer–dimer arrangement, Acta Crystallogr. Sect. D 63 (2007) 581–586.
[19] D.N.P. Doan, T. Dokland, Structure of the nucleocapsid protein of porcine reproductive and respiratory syndrome virus, Structure 11 (2003) 1445–1451.
[20] M.S. Spilman, C. Welbon, E. Nelson, T. Dokland, Cryo-electron tomography of porcine reproductive and respiratory syndrome virus: organization of the nucleocapsid, J. Gen. Virol. 90 (2009) 527–535.
[21] L. Whitmore, B.A. Wallace, DICHROWEB, an online server for protein secondary structure analyses from circular dichroism spectroscopic data, Nucleic Acids Res. 32 (2004) W668–673.
[22] H.M. Truong, Z. Lu, G.F. Kutish, J. Galeota, F.A. Osorio, A.K. Pattnaik, A highly pathogenic porcine reproductive and respiratory syndrome virus generated from an infectious cDNA clone retains the *in vivo* virulence and transmissibility properties of the parental virus, Virology 325 (2004) 308–319.
[23] H. Mardassi, B. Massie, S. Dea, Intracellular synthesis, processing, and transport of proteins encoded by ORFs 5 to 7 of porcine reproductive and respiratory syndrome virus, Virology 221 (1996) 98–112.
[24] S.K. Wootton, D. Yoo, Homo-oligomerization of the porcine reproductive and respiratory syndrome virus nucleocapsid protein and the role of disulfide linkages, J. Virol. 77 (2003) 4546–4557.
[25] C. Lee, J.G. Calvert, S.-K.W. Welch, D. Yoo, A DNA-launched reverse genetics system for porcine reproductive and respiratory syndrome virus reveals that homodimerization of the nucleocapsid protein is essential for virus infectivity, Virology 331 (2005) 47–62.
[26] D.M. Crothers, H. Metzger, The influence of polyvalency on the binding properties of antibodies, Immunochemistry 9 (1972) 341–357.
[27] J.F. Maher, D. Nathans, Multivalent DNA-binding properties of the HMG-1 proteins, Proc. Natl. Acad. Sci. USA 93 (1996) 6716–6720.
[28] B.E. Collins, J.C. Paulson, Cell surface biology mediated by low affinity multivalent protein–glycan interactions, Curr. Opin. Chem. Biol. 8 (2004) 617–625.
[29] T. Dokland, The structural biology of PRRSV, Virus Res. 154 (2010) 86–97.
[30] S. Wootton, G. Koljesar, L. Yang, K.-J. Yoon, D. Yoo, Antigenic importance of the carboxy-terminal beta-strand of the porcine reproductive and respiratory syndrome virus nucleocapsid protein, Clin. Diagn. Lab. Immunol. 8 (2001) 598–603.
[31] D. Yoo, S.K. Wootton, G. Li, C. Song, R.R. Rowland, Colocalization and interaction of the porcine arterivirus nucleocapsid protein with the small nucleolar RNA-associated protein fibrillarin, J. Virol. 77 (2003) 12173–12183.